Manuscript

Phase Sensitive Spectral De-Convolution in Electrophoretic NMR – How to Investigate Neutral Molecules in Lithium Salt-Ionic Liquid Electrolytes

Florian Schmidt[a], Andrea Pugliese[b], Franca Castiglione[b], Catherine Santini[c], Monika Schönhoff[a]*

[a]*Institute of Physical Chemistry, University of Muenster, Corrensstr. 28/30, 48149 Münster, Germany*

Politecn Milan, Dept Chem Mat & Chem Engn Giulio Natta, via Mancinelli 7, I-20131 Milano, Italy

[c]*Université de Lyon, Institut de Chimie de Lyon, UMR 5265 CNRS-C2P2, 43 Boulevard du 11 Novembre 1918, 69616 Villeurbanne, France, catherine.santini@univ-lyon1*

Keywords: phase analysis, spectral analysis, Lorentz fits, lithium transport, PFG-NMR

TOC:

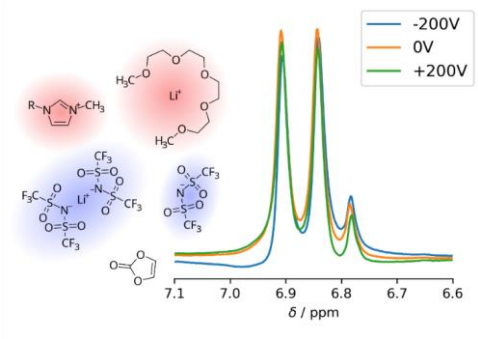

Abstract

Electrophoretic NMR has recently proven to be a powerful tool in studies of nonaqueous electrolytes, such as ionic liquids. It can separately monitor electrophoretic mobilities of various ionic constituents in an electric field, and thus shed light on ion correlations, which determine the conductivity. In applications of liquid electrolytes often uncharged additives are employed, which are accessible via ^{1}H NMR. Characterizing their mobility - and thus their potential coordination to charged entities - is desirable, however often hampered by small intensities and ^{1}H signals overlapping with major constituents of the electrolyte. In this work, we evaluate methods of phase analysis of overlapping resonances to yield electrophoretic mobilities even for minor constituents. We use phase-sensitive spectral de-convolution via a set of Lorentz distributions for the investigation of the migration behavior of additives in two different ionic liquid-based lithium salt electrolytes. Using vinylene carbonate (VC) as an additive, no field-induced drift is observed, thus the additive does not show a coordination-induced correlated drift with the Li^{+} ion. On the other hand, in a solvate ionic liquid with tetraglyme (G4) as an additive, a correlated migration of tetraglyme with lithium as a complex solvate cation is directly shown for the first time. The phase evaluation procedure of superimposed resonances thus broadens the applicability of electrophoretic NMR to application-relevant complex electrolyte mixtures containing different additives with superimposed resonances.

Commentato [CS1]: this sentence has been rewritten, because this is contrary to our results but also to the results of several authors.

Commentato [PDMS2R1]: You probably mean: Sentence has TO BE rewritten?
I think this sentence does not pose a contradiction to your results. The coordination of VC to Li is present, but it is too short-lived to lead to a joint drift motion over a range of µm – which is what we detect in eNMR.
We try to detail this in context with the lifetimes of coordinate bonds in the text.
If you then still see a contradiction, please specify.

Introduction

The electrolyte plays a crucial role for the performance of a battery. Its properties influence important aspects such as battery safety, coulomb efficiency and/or operating temperatures. The very demanding requirements concerning battery electrolytes in modern technologies led to a variety of approaches towards new types of electrolytes.[1-2] With the aim to resolve safety issues, less volatile/flammable liquid electrolytes based on ionic liquids (IL) were considered. However, these electrolytes consisting of a Li salt in an IL usually suffer from high viscosities and low conductivities. In order to improve their properties, neutral additives are employed with the intention of either improving the electrode-electrolyte interface (solid electrolyte interface, SEI), or advancing the lithium transport by weakly coordinating molecules, which compete with the Li-anion interaction. A variety of studies on the impact of additives on the lithium dynamics in ionic liquid electrolytes have been carried out using NMR, electrochemical methods and molecular dynamics simulation techniques.[3-9] Impedance measurements deliver the total conductivity, which can be a first indication of electrolyte performance. However, they do not distinguish between the contributions from different charge carriers. Diffusion NMR measurements, on the other hand, deliver ion-specific information. Assuming validity of the Nernst-Einstein equation, transference numbers and thus the contributions of particular ion species to the conductivity can be determined.[10-12] In concentrated electrolytes, however, ion correlations such as for example ion pair formation may play a large role, as has been shown for a range of different systems.[13-17] In that case, the information content of diffusion coefficients is limited, and in order to take into account different species such as single ions, pairs, or clusters with their various contributions to diffusivity and conductivity, respectively, additional models have to be employed.[18]

Recently, electrophoretic NMR (eNMR) was introduced to the field of Li battery electrolytes.[13, 19] It provides the ability to directly investigate the migration velocities of charged and neutral molecules in an electric field and benefits from the species selectivity that comes with NMR spectroscopy.[20-21] Typically, the investigated nuclei in battery electrolytes are ^{7}Li, ^{1}H contained in the solvent and/or the IL cation, and ^{19}F contained in the investigated anion. The eNMR experiment consists of a pulsed-field-gradient (PFG) NMR diffusion experiment with additional simultaneous electric field pulses applied to the investigated sample. The application of the electric field causes a coherent displacement of the investigated nuclei resulting in a phase shift ϕ-ϕ_0 of the observed NMR signal compared to the signal without electric field.[20, 22]

With this technique, Li transference numbers in IL were determined without assumption of an ideal electrolyte, i.e. assuming validity of the Nernst-Einstein equation. A large influence of Li-anion correlations was found, which even results in an unintended lithium migration in the "wrong" direction caused by strong lithium-anion correlations leading to the transport of net negatively charged clusters.[23-26] This was termed a 'vehicle mechanism' of Li transport, and observed in several salts,[23] and recently confirmed by simulations.[25]

As drift velocities become experimentally accessible, the role of uncharged additives in IL-based electrolytes is interesting to clarify. However, due to typically low concentrations, low mobilities and overlapping signals from different compounds, this has not been attempted so far.

In dilute aqueous salt solutions, however, where experimentally observable phase shifts can reach > 1000°,[22] eNMR was applied to the investigation of multiple molecular species, which exhibit different phase shifts in the ^{1}H eNMR spectrum.[22, 27-29] It was shown that the mobilities can be analyzed via 2D Fourier transformation applying the States-Haberkorn correction yielding a mobility ordered spectrum (MOSY).[22, 30] This has been demonstrated by resolving superimposed ^{1}H eNMR spectra of e.g. aqueous amino acid mixtures or polyelectrolytes and their counterions by their electrophoretic mobilities.[28, 31-35] However, the resolution in the mobility dimension is highly dependent on the mobility difference of the investigated distinct molecular species as well as the observed phase range. When investigating ILs, the observable phase range is significantly less than in aqueous systems due to lower mobilities and higher conductivities limiting the applicable electric fields.[13, 19] Additionally, the electrodes in the NMR sample tube significantly disturb the homogeneity of the static magnetic field and decrease the spectral resolution. Thus, the ability to calculate MOSY spectra from eNMR measurements of ILs is limited.

In the present work, we introduce the phase sensitive spectral de-convolution of eNMR spectra in order to investigate the correlated migration behavior of additives in IL-lithium salt mixtures and to overcome spectral and phase resolution issues. ^{1}H eNMR measurements are performed on two different IL-based lithium salt electrolytes with either added vinylene carbonate (VC) or tetraglyme (G4).). The first mixture consists of 1 mole·L^{-1} LiTFSA in C_1C_6ImTFSA + 5 % (per volume) VC, *i.e* $Li(C_1C_6Im)_3(TFSA)_4(VC)_{0.8}$ which was investigated in the past by NMR spectroscopy, diffusion experiments, and molecular dynamics simulations.[8] The second mixture consists of the solvate ionic liquid $Li(G4)_1TFSA$[36-37] and the Ionic Liquid C_1C_2ImTFSA at a molar ratio of 1:8 resulting in the sum formula $Li(G_4)_1(C_1C_2Im)_8TFSA_9$. Considering previous work on solvate ionic liquids, one expects the

formation of a complex solvate cation effectively breaking unwanted lithium-anion clusters. The ^{1}H eNMR of these mixtures exhibit superimposed ^{1}H NMR signals of the respective imidazolium-based cation and the additive. We compare the results of the proposed deconvolution method to MOSY 2D FFT processed spectra and discuss the applicability of zero order phase correction for phase analysis. Finally, we achieve the determination of the mobilities of additives, even if they are present in minor amounts, and even if ^{1}H resonances are overlapping. We can showcase a system with and without pronounced additive drift, respectively. This first determination of additive mobilities opens the route for studies of the transport of additive species in further electrolyte formulations.

Experimental

Materials

5 vol% of vinylene carbonate (VC, Aldrich >99%) was added to a mixture of 1 mol·L^{-1} lithium bis-(trifluoromethanesulfonyl)amide (LiTFSA, Sigma Aldrich ≥99%) in 1-hexyl-3-methylimidazolium bis-(trifluoromethanesulfonyl)amide (C_1C_6ImTFSA). C_1C_6ImTFSA was synthesized by Bolimowska et al. as reported previously.[8] LiTFSA, tetraethylene glycol dimethyl ether (tetraglyme, G4, Sigma Aldrich ≥99%) and 1-ethyl-3-methyl-imidazolium bis-(trifluoromethanesulfonyl)amide (C_1C_2ImmTFSA, Iolitech ≥99%) were mixed with a molar composition of $Li(G_4)_1(C_1C_2Im)_8TFSA_9$.

Electrophoretic NMR experiments

Experimental data was acquired on a 400 MHz Bruker Avance III HD, equipped with a Diff50 probe head, and a 400 MHz Bruker Avance spectrometer equipped with a Diff30 probe head. A double stimulated echo pulse sequence with gradient pulses[38] was used while applying alternating electric field pulses with an in-house built power source. The electric fields were incremented from low to higher voltages while keeping all parameters of the pulse program constant. The observation times (Δ) were between 100 and 200 ms and the gradient pulse duration (δ) was between 0.5 and 3 ms, depending on the investigated nucleus. A customized sample cell, based on the cylindrical design of Holz,[20] was employed equipped with capillaries and palladium electrodes spaced at a distance of 22 mm as described earlier.[13] The capillaries and the sample cell were dried at high vacuum and 105 °C overnight prior to filling the tube with electrolyte solutions in an argon filled glove box. The ^{1}H chemical shift was

referenced to 8 ppm for the ^{1}H signal of the C^{2} carbon atom of the imidazolium ring in $C_1C_2ImIm^+$, as it was determined for an imidazolium based IL with the TFSA counter ion.[39]

Data evaluation

The python modules nmrglue[40], lmfit, matplotlib, numpy and pandas were used for the import, processing and fitting of all results. For the MOSY processing, zerofilling up to 32k data points in the indirect dimension was applied and the peak height determined by selecting the highest data point.

Phase Analysis Methods

eNMR measurements yield spectra with a phase shift depending on the drift velocity of the respective ion species. This phase shift is directly proportional to the gyromagnetic ratio γ, the magnetic field gradient pulse duration δ and strength g, the observation time Δ and the drift velocity $v_{\pm}$ (see eq. 1). The velocity of the observed nucleus is directly proportional to the applied electric field E and its electrophoretic mobility μ as depicted in eq. 2.

$$\phi - \phi_0 = \gamma \delta \Delta g v_{\pm} \quad (1)$$

$$v_{\pm} = \mu E \quad (2)$$

The phase shift $\phi - \phi_0$ needs to be quantified in order to derive the observed nuclei's mobility. Generally, the phase angle ϕ of a spectrum is defined by eq. 3 where S_0 is the amplitude, $A(\omega)$ the absorptive and $D(\omega)$ the dispersive spectrum.

$$S(\omega) = S_0[A(\omega) + iD(\omega)]exp(i\phi) \quad (3)$$

The simplest approach towards determining ϕ is to multiply the acquired spectrum with $\exp(i\phi_{corr})$ varying ϕ_{corr} until $\phi = -\phi_{corr}$, such that the exponential term in eq. 3 becomes zero, obtaining a purely absorptive spectrum.[41] This process of "phasing" the spectrum is usually done manually under visual inspection of the resulting spectrum. For the series of spectra with individual phases acquired in eNMR, this procedure is time consuming and limited in its accuracy due to a personal bias. In addition, this approach is limited to spectra consisting of single resonances without any superposition by other resonances with a different phase shift. Regarding phase correction, one distinguishes between zero and first order phase correction, in order to correct frequency-independent and frequency-dependent phase

distortions. In the context of eNMR, typically only zero order phase correction is applied to extract ϕ_{corr} from the phase value required to obtain a purely absorptive spectrum.

In order to overcome the drawbacks of manual phase determination, we describe in the following three different approaches towards analyzing the signal phase shift. Furthermore, we compare them with regard to their performance in electrophoretic NMR measurements investigating nuclei with low mobilities.

Entropy Minimization

A variety of phase correction algorithms was introduced in the past in order to automatize and improve the phasing process of NMR spectra.[42-45] The algorithm applied in this work was described as a robust method for phase correction of NMR spectra by Chen et al.[46] It involves an entropy minimization via phase correction, based on the fact that purely absorptive spectra exhibit lower entropies than purely dispersive spectra and therefore the entropy serves well as a quantity to be optimized resulting a in a purely absorptive spectrum. As suggested in the paper by Chen, the first derivative of the spectrum is calculated numerically and consecutively its entropy S is calculated *via* eq. 4. The resulting entropy is then minimized via the Levenberg-Marquardt algorithm by performing zero order phase correction as discussed above.

$$S = -\sum_i h_j \ln h_j \tag{4}$$

The application of zero order phase correction as a tool for the analysis of signal phase shifts requires that the investigated NMR spectrum consists only of a single component exhibiting a single mobility. In particular, it is not possible to distinguish between different phase shifts of superimposed signals. Therefore, this method is not further considered for the analysis of superimposed eNMR spectra.

2D Fast Fourier Transformation (MOSY)

Applying the Euler formula to eq. 3 and inserting eq. 1 and 2 results in eq. 5. It becomes clear that the phase shift of the observed NMR signal can be described as an oscillation of the signal intensity in dependency of the applied electric field E, electrophoretic mobility μ, observation time Δ, gradient strength g and the gradient duration δ.

$$S(\omega) = S_0[A(\omega) + iD(\omega)][cos(\gamma\delta\Delta g\mu E) + isin(\gamma\delta\Delta g\mu E)] \tag{5}$$

Therefore, the electrophoretic mobility can be analyzed via 2D Fourier transformation in the time domain and the electric field domain E, applying a modification of the States-Haberkorn method as applied in

various reports.[22,27-29] The States method is applied to obtain pure absorption phase spectra and suppress phase twist line shapes.[30] For its application, the voltage must be incremented linearly, covering both positive and negative voltage regions.

The data for each frequency ω is then transformed individually without any correlation between frequencies. Due to the nature of Fourier transformation, the resolution of the resulting MOSY spectrum is strongly depending on the number of oscillation periods recorded in the indirect dimension. Unfortunately, the observable phase shift range in eNMR measurements of viscous, highly concentrated solutions is often limited to $<\pi/2$. This minor phase shift results in a poorly resolved MOSY spectrum in the mobility domain. The mobility spectrum may be further broadened due to phase errors caused by experimental artifacts such as electroosmosis or sample decomposition which are difficult to identify in the resulting MOSY spectrum.[47]

Fitting of Lorentz Profiles

Alternatively, for the analysis of phase modulations in eNMR measurements a phase sensitive spectral de-convolution of eNMR spectra can be performed. The benefit of this approach is to extract more precise phase information by correlating data from all frequencies ω, which belong to the same signal, and therefore must exhibit the same phase shift. A limitation of this approach is that an assumption of a particular lineshape is necessary; here, we employ a set of Lorentzian profiles.

The absorptive $A(\omega, \omega_L, \lambda)$ and dispersive Lorentz profile $D(\omega, \omega_L, \lambda)$, depending on the nuclei's resonance frequency ω_L, and the coherence decay rate constant λ which is proportional to the peak width λ/π, are given in equ. (6).

$$A(\omega,\omega_L,\lambda)=\frac{\lambda}{\lambda^2+(\omega-\omega_L)^2};\ D(\omega,\omega_L,\lambda)=\frac{-\omega-\omega_L}{\lambda^2+(\omega-\omega_L)^2} \qquad (6)$$

The real R_i and imaginary I_i part of a NMR spectrum are then given as a trigonometric combination of absorptive and dispersive Lorentzians according to equation 7a and 7b with a as the amplitude and ϕ as the signal phase. In the case of $\phi = 0$, one obtains a purely absorptive R_i and a purely dispersive I_i spectrum.[41]

$$R_i=|a|(A(\omega,\omega_L,\lambda)cos\phi-D(\omega,\omega_L,\lambda)sin\phi) \qquad (7a)$$
$$I_i=|a|(D(\omega,\omega_L,\lambda)cos\phi+A(\omega,\omega_L,\lambda)sin\phi) \qquad (7b)$$

For the analysis of an eNMR data set, each recorded spectral row corresponding to an applied voltage is approximated individually via the sum of a set of Lorentzians. The complex phase sensitive spectral function is given by equation 8, where n_p is the number of peaks to be fitted, b the baseline and ω_i, λ_i, a_i and ϕ_i are individual parameters for each fitted peak according to equation 6.

$$\hat{S}(\omega, \omega_i, \lambda_i, a_i, \phi_i, b) = b + \sum_{i=1}^{n_p} [R_i(\omega, \omega_i, \lambda_i, a_i, \phi_i) + iI_i(\omega, \omega_i, \lambda_i, a_i, \phi_i)] \qquad (8)$$

In order to reduce the degrees of freedom of the fit model, reasonable restrictions to the fit function may be introduced, *e.g.* using the same phase ϕ_i for peaks which are assigned to the same molecule and therefore will exhibit the same signal phase shift.

This approach correlates all frequencies with each other and considers physically meaningful dependencies of correlated resonances, while being able to describe superimposed signals. Contrary to MOSY processing, the individual phase values for each electric field value E are obtained which makes it easier to test their linearity and thus identify potential experimental artifacts.

Results & Discussion

Vinylene carbonate in LiTFSA/C_1C_6ImTFSA

The mixture of VC with 1 mole·L^{-1} LiTFSA in C_1C_6ImTFSA was investigated via ^{1}H, ^{7}Li and ^{19}F eNMR. In the ^{1}H spectrum, the low VC concentration results in only a minor VC signal, which is furthermore overlapping with the ^{1}H resonances of the $C_1C_6Im^+$ (see supplementary material, figure S1). Two regions of the full ^{1}H eNMR spectrum were selected for the analysis of the $C_1C_6Im^+$ and VC mobilities. The first region exhibits the C^4 and C^5 ^{1}H signals (8.2 – 6.6 ppm) of the organic cation's imidazolium ring as well as the ^{1}H signal of VC, whereas the second region (2 – -0.5 ppm) exhibits solely isolated alkyl ^{1}H signals of $C_1C_6Im^+$ and serves as reference for the Lorentz fitting method. The ^{1}H spectra of the VC region acquired with -200, 0 and +200 V are depicted in figure 1 exhibiting only minor phase variations which could be mistaken for random phase errors. However, it is not apparent from this depiction whether all three peaks exhibit the same or deviating phase shifts, respectively.

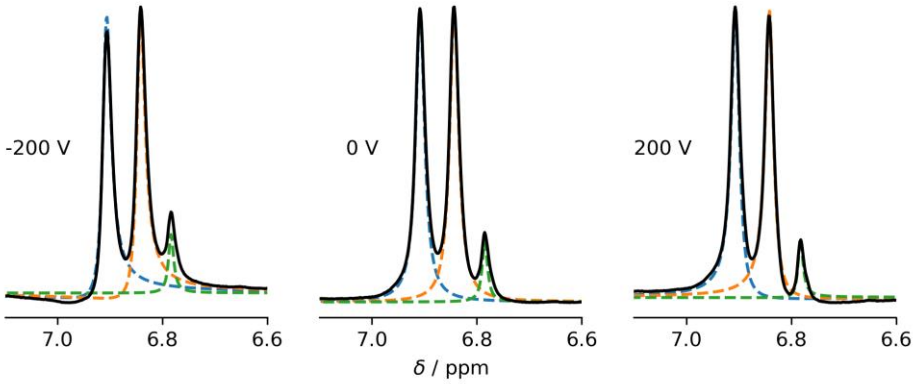

Fig 1: Spectral region of the ^{1}H eNMR spectra of VC/C_1C_6ImTFSA/LiTFSA containing the $C^{4/5}$ ^{1}H signals of the imidazolium ring and the smaller VC signal at -200, 0 and 200 V, dashed lines: Lorentzian fits (VC: green dashed line).

MOSY

The ^{1}H MOSY spectrum was calculated for the first spectral region (8.2 – 6.6 ppm) containing the VC signal of the investigated VC/LiTFSA/C_1C_6ImTFSA mixture and is shown in figure 2 a). The two peaks labelled as $C^{4/5}$ correspond to the adjacent aromatic protons in $C_1C_6Im^+$ while VC corresponds to the

proton signal in vinylene carbonate. Only a very minor distinction between the $C^{4/5}$ and VC signals can be made in the mobility dimension of figure 2 a).

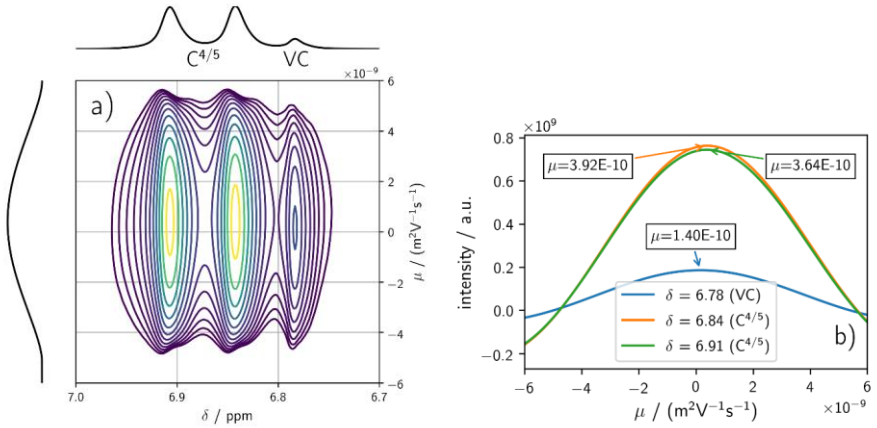

Fig 2: a) ^1H MOSY of spectral VC and $C^{4/5}$ region b) Slices of the ^1H MOSY spectrum at $C^{4/5}$ (δ = 6.91 ppm and δ = 6.84 ppm) and VC (δ = 6.78 ppm) peaks.

Commentato [PA3]: If and/or when it is possible, it should be great to have a sort of "color-code" in figures.
For example, according to Figure 1, in the paper all the fitting curves related to VC should be green, curves for peak at 6.84 ppm be in orange, and finally curves for the signal at 6.91 ppm could be blue.

Slices of the MOSY spectrum corresponding to the chemical shifts of the discussed signals are extracted, see figure 2 b), in order to obtain a better comparison of the peaks of interest and the mobility differences. Electrophoretic mobilities obtained from the respective maxima are indicated in figure 2 b). Both $C^{4/5}$ signals (δ: 6.91 and 6.84 ppm), exhibit approximately the same mobility but deviate from each other by approximately $0.3 \cdot 10^{-10} m^2V^1s^{-1}$. VC exhibits a peak maximum at $1.4 \cdot 10^{-10} m^2V^1s^{-1}$. However, this maximum is very broad, indicating a considerable error. In addition, considering the low intensity the overlapping $C^{4/5}$ signals may influence the position of the maximum. Thus, while both $C^{4/5}$ signals are clearly occurring at positive mobilities, it is hard to state whether the small positive value of VC is an overlap-induced artefact, or indicates a true drift of VC. Thus, the analysis of MOSY processed eNMR is limited in this application.

Lorentz fitting procedure

Both spectral regions were fitted individually with a superposition of three Lorentzians. For the first spectral region (7.1 – 6.6 ppm) examples of the fit are shown in figure 1 by dashed lines. Here, the phase, amplitude and peak width of the two $C_1C_6Im^+$ signals were set to identical values, respectively. For the fit of the second spectral region (2 – -0.5 ppm), the phase was set equal for all isolated ^1H alkyl signals.

These physically meaningful restrictions to the fit models were introduced in order to reduce the degrees of freedom by correlating not only frequencies of a single signal but of multiple signals which belong to the same molecular species.

The phase shift values obtained for the superimposed VC and $C_1C_6Im^+$ signals are depicted in figure 3a) and clearly deviate from each other. The second spectral region was analyzed as well by spectral deconvolution, resulting in the phase data in figure 3b), see full blue circles. For comparison, we also performed an analysis via phase correction, these data (open circles in figure 3b) show very good agreement with the fit results, showing that the described phase correction method and the fitting method yield equivalent results, if no superposition is present. In addition, the phase shift values of $C_1C_6Im^+$ depicted in 3a) and 3b) are in very good agreement, validating the fit of the superimposed $C^{4/5}$ and VC signals. The $C_1C_6Im^+$ mobility obtained from the superimposed fit of the $C^{4/5}$ signals in the first spectral region containing the ^1H VC signal is $(4.1 \pm 0.2) \cdot 10^{-10}$ $m^2V^{-1}s^{-1}$, it matches very well the mobilities obtained from the second spectral region (2 – -0.5 ppm) analyzed via phase correction, $(4.3 \pm 0.2) \cdot 10^{-10}$ $m^2V^{-1}s^{-1}$, and the mobility extracted by Lorentz fitting, which is $(4.2 \pm 0.2) \cdot 10^{-10}$ $m^2V^{-1}s^{-1}$.

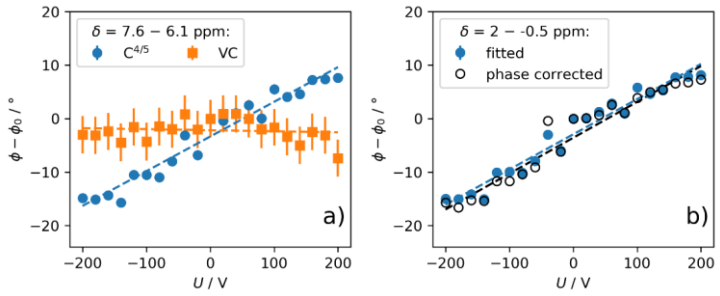

Fig 3: Phase shift values ϕ-ϕ_0 plotted against the applied voltages obtained from a) fit results of the superimposed VC and $C^{4/5}$ signals observed between 7.6 and 6.1 ppm. b) Fitted and phase corrected phase shift values of the isolated aliphatic ^1H $C_1C_6Im^+$ signals observed between 2 and -0.5 ppm.

While $C_1C_6Im^+$ exhibits a positive slope and therefore a positive mobility, this is not the case for VC with $\mu = (-0.1 \pm 0.2) \cdot 10^{-10}$ $m^2V^{-1}s^{-1}$. However, the error bars of the phase shifts of VC are large since the VC signal contributes only to a small part of the fitted region. Hence, one can conclude that VC has either a very low negative, but more likely an electrophoretic mobility of zero. Note that this result does not agree with the value extracted from the MOSY spectrum, probably the influence of the adjacent $C^{4/5}$ resonance with its large positive mobility is influencing the phase of the VC signal.

Finally, the zero mobility of VC sheds light on the influence of solvent coordination on Li^+ migration: Previously, ^7Li-^1H HOESY experiments have indicated a vicinity of VC with Li^+ and MD results suggest an average contribution of 0.5 O_{VC} atoms in the first Li^+ solvation shell.[8] Thus, a coordination of VC to Li^+ is clearly evident. On the other hand, this coordination is not sufficiently long-lived to induce a drag of VC alongside with Li^+ in the electric field.

Concerning the Li^+ transport, for Li salt-in-IL systems without additive it was previously discussed whether the Li^+ transport may occur as structural transport via Li^+ ion hopping between different coordination sites (involving short-lived Li-anion coordinations), or via a vehicle transport of Li-containing clusters, involving a Li-anion coordination lifetime, which is longer than the time scale of a cluster displacement.[Gouv 18, Bri 19] There, long-lived coordinations were found, leading to vehicle transport of $Li(Anion)_x^{1-x}$ clusters, evidenced by a negative transference number of Li.[Gou 18] In the present system, containing VC, we also investigated the Li^+ migration by ^7Li eNMR, see figure S2 in the Supplementary Material. The results show a negative Li^+ mobility, similar to the findings in salt-in-IL systems without added carbonate.[23] Hence, the Li^+ migration behavior is still dominated by anionic lithium-anion clusters.

Concerning the VC-Li^+ coordination, the opposite case applies: A short-lived VC-Li coordination leads to Li^+ moving between different VC coordination sites, which do not experience a drift in the electric field, while Li^+ still drifts alongside with its coordinated anions in the anion direction. The correlated motion with the anions might be, however, reduced by the VC coordination, which is possibly the cause for the improved performance of lithium-ion batteries using ionic liquid electrolytes with VC.[18] ~~is thus rather driven by other improvements to the chemistry of the electrolyte then by an improved/altered lithium migration mechanism~~.

Commentato [CS4]: **Due to the overlapping of the peaks and the difficulties that you met to extract the values concerning VC I would propose a less categorical conclusion to the role of VC. I am not expert in nmr, but an interaction between VC and Li has been evidenced by HETCOR experiments. How could explain this difference? See above commentary are we observing phenomena in the same time range ?**

Other comment In LiG4 the G is already coordinated to Li cation,(structure of the LiG4TFSA) while LiTFSA in IL is coordinated to at least 2 to 3 TFSA 2 bidentate one monodentate. Kinetic rate of the ligand exchange??

Commentato [PDMS5R4]: First comment: The coordination is clearly evident, but not long-lived enough. Does the extension of the passage in Yellow clarify this point sufficiently?
The statement has been altered.

Other comment: Yes, the difference lies in the lifetimes.
Li-glyme: Long lifetime → joint drift
Li-FSA: long lifetime only without glyme, but with glyme short lifetime of Li-anion coordination
Is it clear now?

$Li(G4)_1(C_1C_2Im)_8TFSA_9$

The system of $Li(G_4)_1(C_1C_2Im)_8TFSA_9$ offers another example to showcase the analysis of superimposed ^1H eNMR spectra via phase sensitive spectral de-convolution. In this mixture, the tetraglyme (G_4) is coordinated to the lithium ion forming a complex cation. Therefore, a non-zero electrophoretic mobility might be expected for G_4, despite it does not carry a charge itself. Again, two regions of the ^1H eNMR

spectrum (see the full spectrum in figure S3) are selected. Figure S4 shows spectra of these regions taken with the double stimulated echo sequence at different voltage values of the electric field pulse. The first spectral region (8.5 – 6.5 ppm) exhibits only the aromatic proton signals of $EMIm^+$ while the second region (4.2 – 2.5 ppm) exhibits a superimposed spectrum of the G_4 signals and the aliphatic proton signals of $C_1C_2Im^+$.

MOSY

The MOSY processed data of the second spectral region of $Li(G_4)_1(C_1C_2Im)_8TFSA_9$ is depicted in figure 4a). All $C_1C_2Im^+$ and G_4 signals exhibit a shift towards positive mobilities μ with a large uncertainty due to the poor mobility resolution. However, one can conclude from the MOSY spectrum that the signals E^1 and E^2 represent a higher electrophoretic mobility than G^1, G^2 and G^3.

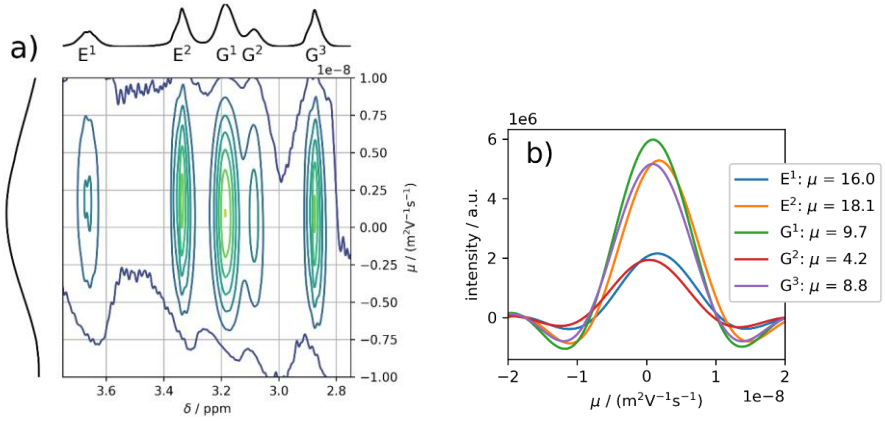

Fig 4: a) ^1H MOSY of the spectral region with superimposed G_4 and $C_1C_2Im^+$ signals. The peaks E^1 and E^2 correspond to $C_1C_2Im^+$, while the peaks G^1, G^2 and G^3 are assigned to tetraglyme (G4) b) Slices of the MOSY spectrum through the peak maxima of E^1, E^2, G^1, G^2 and G^3. The mobilities μ obtained from the peak maxima are given in the legend in $10^{-10}m^2V^1s^{-1}$.

Slices of the MOSY peaks E^1, E^2, G^1, G^2 and G^3 in the mobility dimension are presented in figure 4 b). This depiction emphasizes the different intensities of the MOSY signals. The legend gives the corresponding mobility for each peak in 10^{-10} $m^2V^1s^{-1}$. The mobilities assigned to $C_1C_2Im^+$ are significantly higher (16.0 and 18.1)$\cdot 10^{-10}m^2V^1s^{-1}$ than those of G4 (9.7, 4.2 and 8.8)$\cdot 10^{-10}m^2V^1s^{-1}$). The deviation between the mobilities obtained for the same molecule, but from different resonances gives an

estimate for the uncertainty of this method. It appears that the peaks with lower intensities tend to result in lower mobilities than their counterparts of the same compound. Furthermore, the G^1 peak exhibits a higher mobility compared to the G^3 peak with a similar intensity. This is most likely due to its slight superposition with the E^2 peak and the resulting partial superposition of oscillations. Thus, even in this second example, MOSY is not a precise and reliable analysis method for the analysis of eNMR measurements on ionic liquids.

Lorentz fitting procedure

Phase sensitive spectral de-convolution of the ^{1}H eNMR spectra of $Li(G_4)_1(C_1C_2Im)_8TFSA_9$ was performed on both spectral regions. The first region, containing only $C_1C_2Im^+$ resonances, results in the phase values given by the black circles in Fig. 5b). The second region, exhibiting the superimposed $C_1C_2Im^+$ and G_4 signals, was fitted with and without restrictions to the fit model in order to test the necessity of physically meaningful restrictions. Figure 5 a) gives the results of fits without any restrictions, and Fig. 5 b) results for fits with the phases set equal for peaks that correspond to the same compound. In figure 5 a), the phase shifts of the G^2 peak are not in good agreement with the G^1 and G^3 peak. This is physically not meaningful since all three signals belong to the same molecular species. Hence, some restrictions the fit model are necessary in order to obtain reasonable results. In figure 5b), the phase shifts of the isolated $C_1C_2Im^+$ signals are in very good agreement with those analyzed in a superposition with the G4 signals. Both exhibit the same phase shift values ϕ-ϕ_0 resulting in a $C_1C_2Im^+$ mobility of $(14.6 \pm 0.3) \cdot 10^{-10} m^2V^{-1}s^{-1}$. This shows that the determination of the $C_1C_2Im^+$ phase shift in the superimposed spectrum is accurate.

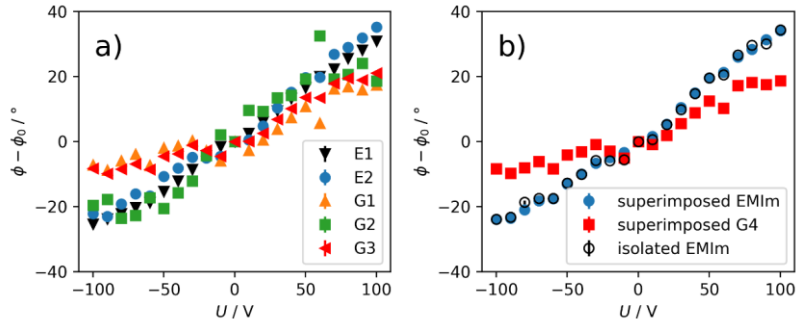

Fig 5: Phase shift values ϕ-ϕ_0 against the applied voltage obtained from superimposed ^{1}H eNMR spectra (δ = 4.2 – 2.5 ppm) of $Li(G4)_1C_1C_2Im_8TFSA_9$ using a) an unrestricted fit model and b) physically

Commentato [PA6]: Also here, the colors for E1, E2, G1, G2, G3 curves could be the same as reported in fig 4

meaningful model restrictions for the phase-sensitive spectral de-convolution method. The phase shift values of the analyzed isolated $C_1C_2Im^+$ signals (δ = 8.5 – 6.5 ppm) are depicted in b).

The phase shift values of G_4 obtained from the same superimposed fit model exhibit a shallower slope resulting in a mobility of $(7.2 \pm 0.5) \cdot 10^{-10} m^2V^{-1}s^{-1}$. Interestingly, this G_4 mobility agrees well with the lithium mobility of $(7.4 \pm 0.7) \cdot 10^{-10} m^2V^{-1}s^{-1}$ extracted from ^{7}Li eNMR experiments on the same sample (see phase shifts in fig. S5). Thus, a correlated migration of G_4 with lithium in form of $(LiG_4)^+$ solvate ions can be concluded in $Li(G_4)_1(C_1C_2Im)_8TFSA_9$. Previous studies had already suggested the correlated migration of G4 with lithium as a complex solvate cation, since identical self-diffusion coefficients were observed.[36-37] Furthermore, the results show that Li^+ is migrating in the expected "right" direction. The coordination with G_4 apparently reduces the lithium-anion interaction and breaks the net negatively charged Li-anion clusters. G_4 thus serves to form a complex solvate cation and effectively reverses the lithium migration from the "wrong" to the "right direction.

Finally, comparing the two systems including VC and glyme, respectively, major difference are obvious, which can be attributed to a very different coordination strength of the respective additive to Li^+: We recall that the additive-free Li salt in IL system exhibits a Li migration in a vehicle mechanism in form of net negatively charged $Li(Anion)_x^{1-x}$ clusters. VC as an additive in such an electrolyte does not change the lithium migration mechanism direction, though it may weaken the Li-anion coordination somewhat. The vinylene carbonate itself exhibits no significant migration, but is nevertheless coordinated to Li^+, thus these coordination bonds can be concluded to be short-lived. Hence, no long-lived vinylene carbonate lithium-clusters are formed and lithium-anion clusters are still dominating the lithium migration behavior in this mixture.

Tetraglyme, on the other hand, shows a strong coordination to Li^+, and we prove here a migration of these neutral molecules in an electric field. This is attributed to a long-lived coordination, thus Li is dragging the tetraglyme along in the field direction. The Li-glyme clusters effectively act like a cation. In addition, G4 leads to the effective breakage of negatively charge lithium-anion clusters as indicated by a positive lithium mobility.

Commentato [PDMS7]: Additional comparative discussion

Conclusion

Superimposed electrophoretic NMR spectra in combination with limited observable phase ranges result in poorly resolved MOSY spectra which are heavily impacted by the superposition of adjacent signals with different phase shifts. However, this limitation can be overcome by spectral de-convolution of eNMR spectra via a set of Lorentz profiles with absorptive and dispersive components. However, reasonable restrictions need to be introduced to the fit model in order to obtain reliable results. Using this procedure, we could for the first time analyze the transport of uncharged, coordinating solvent molecules in an electric field and reveal correlated or uncorrelated additive-lithium migration, respectively. Instead of indirectly deducing migration behavior from diffusion measurements, we directly observe the displacement of the investigated molecules within an electric field.

Using vinylene carbonate as an additive in a lithium salt-ionic liquid electrolyte does not change the lithium migration mechanism significantly. Lithium is migrating correlated with the anions in net negatively charged clusters, and is thus migrating in the "wrong" direction, while vinylene carbonate exhibits no significant migration. Hence, no long-lived vinylene carbonate lithium-clusters are formed and lithium-anion clusters are still dominating the lithium migration behavior in this mixture.

Commentato [CS8]: I prefer this conclusion

On the other hand, using tetraglyme as the additive in a lithium salt-ionic liquid electrolyte leads to the effective breakage of negatively charge lithium-anion clusters as indicated by a positive lithium mobility. In this context, we observed for the first time the correlated migration of tetraglyme with lithium as a complex solvate cation, which was previously suggested for solvate ionic liquids.

Acknowledgement

We thank Andrea Mele of Polytecnico Milano for valuable discussions and his help in initiating this project.

References

[1] M. Marcinek, J. Syzdek, M. Marczewski, M. Piszcz, L. Niedzicki, M. Kalita, A. Plewa-Marczewska, A. Bitner, P. Wieczorek, T. Trzeciak, M. Kasprzyk, P. Lezak, Z. Zukowska, A. Zalewska, W. Wieczorek, *Solid State Ionics* **2015**, *276*, 107-126.

[2] M. Watanabe, K. Dokko, K. Ueno, M. L. Thomas, *Bull. Chem. Soc. Jpn.* **2018**, *91*, 1660-1682.

[3] P. M. Bayley, G. H. Lane, N. M. Rocher, B. R. Clare, A. S. Best, D. R. MacFarlane, M. Forsyth, *Phys. Chem. Chem. Phys.* **2009**, *11*, 7202.

[4] P. M. Bayley, G. H. Lane, L. J. Lyons, D. R. MacFarlane, M. Forsyth, *J. Phys. Chem. C* **2010**, *114*, 20569-20576.

[5] M. L. P. Le, L. Cointeaux, P. Strobel, J.-C. Leprêtre, P. Judeinstein, F. Alloin, *J. Phys. Chem. C* **2012**, *116*, 7712-7718.

[6] A. Deshpande, L. Kariyawasam, P. Dutta, S. Banerjee, *J. Phys. Chem. C* **2013**, *117*, 25343-25351.

[7] A. Eilmes, P. Kubisiak, *J. Phys. Chem. B* **2015**, *119*, 11708-11720.

[8] E. Bolimowska, F. Castiglione, J. Devemy, H. Rouault, A. Mele, A. A. H. Pádua, C. C. Santini, *J. Phys. Chem. B* **2018**, *122*, 8560-8569.

[9] Z. Li, O. Borodin, G. D. Smith, D. Bedrov, *J. Phys. Chem. B* **2015**, *119*, 3085-3096.

[10] S. Jeremias, M. Kunze, S. Passerini, M. Schönhoff, *J. Phys. Chem. B* **2013**, *117*, 10596-10602.

[11] M. Brinkkötter, E. I. Lozinskaya, D. O. Ponkratov, P. S. Vlasov, M. P. Rosenwinkel, I. A. Malyshkina, Y. Vygodskii, A. S. Shaplov, M. Schönhoff, *Electrochim. Acta* **2017**, *237*, 237-247.

[12] K. Yoshida, M. Tsuchiya, N. Tachikawa, K. Dokko, M. Watanabe, *J. Electrochem. Soc.* **2012**, *159*, A1005-A1012.

[13] M. Gouverneur, J. Kopp, L. van Wüllen, M. Schönhoff, *Phys. Chem. Chem. Phys.* **2015**, *17*, 30680-30686.

[14] M. Kunze, Y. Karatas, H.-D. Wiemhöfer, M. Schönhoff, *Macromolecules* **2012**, *45*, 8328-8335.

[15] J. Popovic, C. Pfaffenhuber, J. P. Melchior, J. Maier, *Electrochem. Commun.* **2015**, *60*, 195-198.

[16] K. Ueno, H. Tokuda, M. Watanabe, *Phys. Chem. Chem. Phys.* **2010**, *12*, 1649-1658.

[17] J. Maier, *Electrochim. Acta* **2014**, *129*, 21-27.

[18] N. A. Stolwijk, J. Kösters, M. Wiencierz, M. Schönhoff, *Electrochim. Acta* **2013**, *102*, 451-458.

[19] Z. Zhang, L. A. Madsen, *J. Chem. Phys.* **2014**, *140*, 084204.

[20] M. Holz, *Chem. Soc. Rev.* **1994**, *23*, 165.

[21] P. C. Griffiths, *Annual Reports on NMR Spectroscopy* **2009**, *65*, 139-159.

[22] U. Scheler, in *Encyclopedia of Magnetic Resonance, Online*, John Wiley & Sons Ltd., **2012**.

[23] M. Gouverneur, F. Schmidt, M. Schönhoff, *Phys. Chem. Chem. Phys.* **2018**.

[24] J. C. Lassegues, J. Grondin, D. Talaga, *Phys. Chem. Chem. Phys.* **2006**, *8*, 5629-5632.

[25] N. Molinari, J. P. Mailoa, B. Kozinsky, *J. Phys. Chem. Lett.* **2019**.

[26] M. Brinkkötter, G. A. Giffin, A. Moretti, S. Jeong, S. Passerini, M. Schönhoff, *Chem. Commun.* **2018**, *54*, 4278-4281.

[27] K. F. Morris, C. S. Johnson, *J. Am. Chem. Soc.* **1992**, *114*, 776-777.

[28] Y. Fang, P. V. Yushmanov, I. Furo, *Magn. Reson. Chem.* **2017**, *55*, 584-588.

[29] Q. H. He, C. S. Johnson, *J. Magn. Reson.* **1989**, *81*, 435-439.

[30] D. J. States, R. A. Haberkorn, D. J. Ruben, *J. Magn. Reson.* **1982**, *48*, 286-292.

[31] U. Böhme, A. Klenge, B. Hanel, U. Scheler, *Polymers* **2011**, *3*, 812-819.

[32] U. Böhme, U. Scheler, *Adv. Colloid. Interfac.* **2010**, *158*, 63-67.

[33] U. Böhme, U. Scheler, *Macromol. Symp.* **2004**, *211*, 87-92.

[34] U. Scheler, U. Böhme, *Abstr. Pap. A. Chem. S.* **2003**, *225*, U631-U631.

[35] S. Wong, U. Scheler, *Colloid Surface A* **2001**, *195*, 253-257.

[36] K. Ueno, K. Yoshida, M. Tsuchiya, N. Tachikawa, K. Dokko, M. Watanabe, *J. Phys. Chem. B* **2012**, *116*, 11323-11331.

[37] K. Yoshida, M. Nakamura, Y. Kazue, N. Tachikawa, S. Tsuzuki, S. Seki, K. Dokko, M. Watanabe, *J. Am. Chem. Soc.* **2011**, *133*, 13121-13129.

[38] A. Jerschow, N. Müller, *J. Magn. Reson.* **1997**, *125*, 372–375.

[39] T. Cremer, C. Kolbeck, K. R. J. Lovelock, N. Paape, R. Wölfel, P. S. Schulz, P. Wasserscheid, H. Weber, J. Thar, B. Kirchner, F. Maier, H.-P. Steinrück, *Chem. Eur. J.* **2010**, *16*, 9018-9033.

[40] J. J. Helmus, C. P. Jaroniec, *J. Biomol. NMR* **2013**, *55*, 355-367.

[41] J. Keeler, *Understanding NMR Spectroscopy*, Wiley, **2011**.

[42] R. R. Ernst, *J. Magn. Reson.* **1969**, *1*, 7-26.

[43] J. Van Vaals, P. Van Gerwen, *J. Magn. Reson.* **1990**, *86*, 127-147.

[44] D. E. Brown, T. W. Campbell, R. N. Moore, *J. Magn. Reson.* **1989**, *85*, 15-23.

[45] A. Heuer, *J. Magn. Reson.* **1991**, *91*, 241-253.

[46] L. Chen, Z. Q. Weng, L. Y. Goh, M. Garland, *J. Magn. Reson.* **2002**, *158*, 164-168.

[47] E. Pettersson, I. Furó, P. Stilbs, *Concept. Magn. Reson. A* **2004**, *22A*, 61-68.

[48] H. Srour, H. Rouault, C. Santini, *J. Electrochem. Soc.* **2013**, *160*, A66-A69.

Supplementary Material

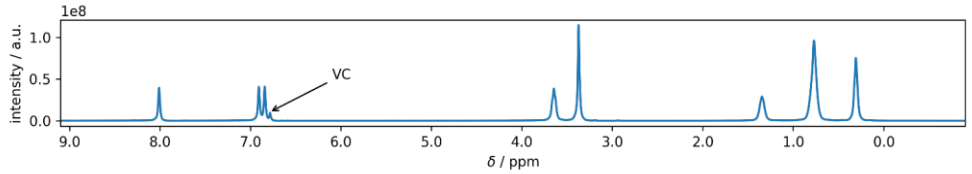

Fig. S1: Full ^{1}H spectrum of the VC/IL/Li-Salt mixture with the the only VC resonance annotated.

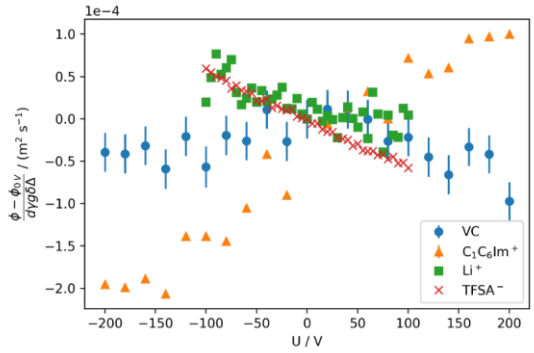

Fig. S2: Reduced phase shifts obtained from ^{1}H and ^{7}Li eNMR measurements of all investigated species in $C_1C_6ImTFSA$ + 1mole.L^{-1} LiTFSA+ 5% VC, i.e $Li(C_1C_6Im)_3(TFSA)_4(VC)_{0.8}$, showing the negative mobilities of $TFSA^-$ and Li^+ indicated by a negative slope, as well as the positive mobility of $C_1C_6Im^+$ indicated by a positive slope.

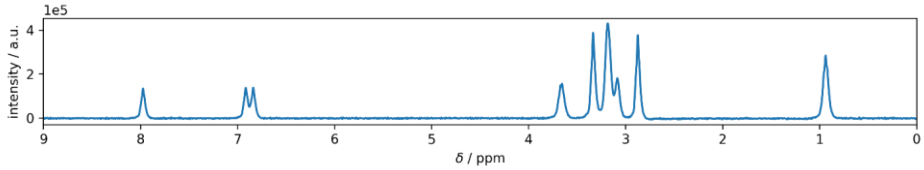

Fig. S3: Full ^{1}H spectrum of the $Li(G_4)_1(C_1C_2Im)_8TFSA_9$ mixture.

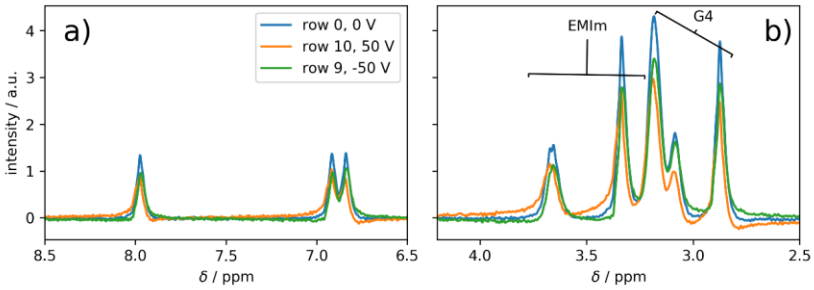

Fig. S4: ^{1}H eNMR spectra recorded at 0, -50 V and +50 V showing the phase modulation in the spectral region a) containing only the aromatic C^{2} and $C^{4/5}$ signals and b) containing aliphatic $C_1C_2Im^+$ signals and the G4 signals.

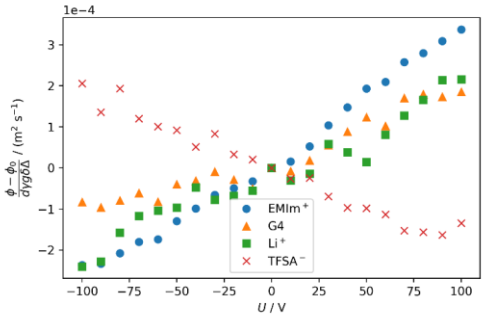

Fig. S5: Reduced, fitted phase shift values of all components in $Li(G_4)_1(C_1C_2Im)_8TFSA_9$ against the applied voltage.